Journal of Catalysis **205,** 107–114 (2002)
doi:10.1006/jcat.2001.3425, available online at http://www.idealibrary.com on IDEAL®

Theoretical Study of NO_2 Adsorption on a Transition-Metal Zeolite Model

Anibal Sierraalta,*[,1] Rafael Añez,* and Marcos-Rosas Brussin†

*Laboratorio de Química Computacional, Centro de Química, Instituto Venezolano de Investigaciones Científicas, Apartado 21827, Caracas 1020-A, Venezuela; and †Centro de Catálisis, Petróleo y Petroquímica, Facultad de Ciencias, Universidad Central de Venezuela, Caracas, Venezuela

Received May 30, 2001; revised September 3, 2001; accepted September 8, 2001

Calculations for the study of NO_2 adsorption on a transition-metal-exchanged zeolite (M = Zn, Cu, Ni, Co, Fe) were carried out using an *ab initio* density functional theory and pseudopotential approaches. A tritetrahedral model (T3) was used to represent the structure of the zeolite. The density functional calculations predict that the bonding energy follows the order Zn > Ni > Cu > Fe > Co. Analysis of the electronic properties shows that only in the case of Cu and Ni ions does the d^{10}-s^1d^9 promotion favor interaction between the NO_2 molecule and the metallic center. The optimization results show that there is a charge transfer from the metallic ion to the NO_2 molecule, which produces a weakening of the N–O bond. © 2002 Elsevier Science

Key Words: **SCR; NO_x adsorption; zeolites; NO_2 reduction; DFT; theoretical study; nitrogen oxides; NO decomposition; ZSM-5; *M*-ZSM-5.**

INTRODUCTION

Environmental pollution caused by chemicals contained in exhaust gases from mobile and stationary sources is a serious problem that needs to be solved. In particular, unwanted pollutants such as nitrogen oxides participate in chemical reactions in the atmosphere and in chemical corrosion such as photochemical smog and acid rain. Currently the NO_x emissions are controlled by the reduction of nitrogen oxides in the presence of O_2 by NH_3 on titania-supported vanadia (1–3). Nevertheless the use of ammonia as a reductant is undesirable because large quantities of ammonia must be stored, and the process must be controlled to avoid its toxic and corrosive effects. On the other hand, the selective catalytic reduction (SCR) of NO_x by hydrocarbons using metal-zeolite catalysts, in which ammonia is not used, has been considered as a practical alternative for the elimination of nitrogen oxide pollutants.

Iwamoto (4–7) and Held *et al.* (8) have reported that the reduction of NO_x by hydrocarbons can be carried out by copper-zeolite catalysts in the presence of oxygen. The copper atoms are introduced into the zeolite (ZSM-5) by ion exchange from a copper(II) acetate solution (7). These copper-exchanged zeolites (Cu-ZMS-5) have shown good catalytic activity (9), and some studies indicate that Cu^+ is the active site of these catalysts (10–14). Along with Cu, other metals have been used to prepare metal-exchanged zeolites, for example, Ce-ZMS-5 (15–18), Co-ZMS-5 (5, 19–23), and the controversial Fe-ZMS-5 (20, 24–27).

Details of the manner in which the NO_2 or NO molecules bind to supported transition metals (TM) or metal oxides in their different oxidation states are not totally known. For example, it is not clear yet what the oxidation state of the active iron in the Fe-ZSM-5 system (25, 27) is. In general, in real catalytic systems there are several states where the size of the cluster species (from isolated ions to monocrystalline aggregates) and the oxidation state of the ions differ. Therefore, adsorption studies as well as interaction energies and charge transfer studies are of particular interest in understanding the mechanisms of NO_2/NO decomposition by TM-zeolites. A fairly large number of publications on this topic (14, 27–37) demonstrate that considerable effort has been devoted to this problem. In spite of this, more experimental and theoretical studies are necessary to fully understand the NO_2 and NO interactions with the different TM-zeolite systems and the elementary steps of the reaction mechanisms.

The present work was undertaken to understand the chemistry associated with the adsorption of NO_2 on supported metals in zeolites. The analysis of the electronic interaction of the NO_2 molecule with different cluster models (M-zeolite: M = Fe, Co, Ni, Cu, and Zn), using *ab initio* Density functional theory calculations is presented.

CATALYST MODELS

Five different M-zeolite systems (M = Zn, Cu, Ni, Co, and Fe) were studied to analyze the electronic properties of NO_2 adsorbed on transition metals supported on a zeolite framework. A trietrahedral model $[H_3SiOAl(OH)_2OSiH_3]^-$, as shown in Fig. 1, was chosen as the T3 site model of the ZSM-5 zeolite, with the metallic atom M set on a bridge between two oxygen atoms. Similar models have been used successfully in the literature (14, 37) to represent

[1] To whom correspondence should be addressed. E-mail: asierral@ivic.ve.

0021-9517/02 $35.00

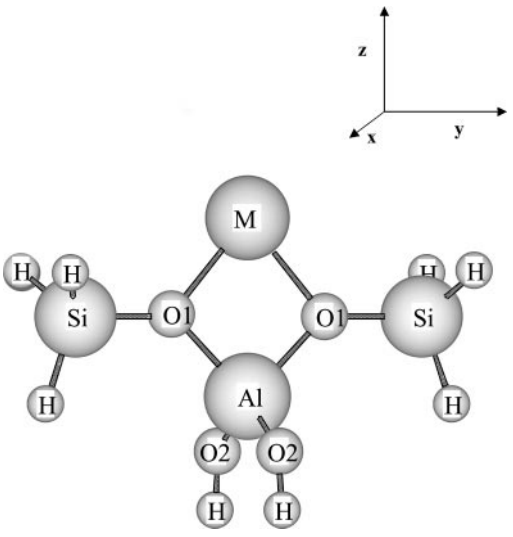

FIG. 1. Schematic representation of the T3 site of the zeolite model used in this work. The O1 atoms are located along the *y* axis. The Al and *M* atoms are in the *z* axis.

one of the possible sites for the location of the metallic ion inside the zeolite framework (36).

THEORETICAL BACKGROUND

In Bader's topological theory, found in "Atoms in Molecules: A Quantum Theory" (AIM) (38–40), the chemical bonds and molecular reactivity can be interpreted in terms of the total molecular electronic density, $\rho(r)$, and its corresponding laplacian, $\nabla^2\rho(r)$. The values of $\rho(r)$ and $\nabla^2\rho(r)$ at the bond critical point (bcp) characterize the chemical bonds of the atoms in the molecules. According to the AIM theory $\nabla^2\rho(r)$ provides information concerning electronic charge, where $\nabla^2\rho(r) > 0$ (or $-\nabla^2\rho(r) < 0$) implies a locally depleted charge, while, in contrast $\nabla^2\rho(r) < 0$ (or $-\nabla^2\rho(r) > 0$) signifies a locally concentrated charge (38–39). Thus, classical covalent bonds or shared interactions have values at the bcp of $\nabla^2\rho_{bcp} < 0$ and high ρ_{bcp}, while classical ionic bonds (closed-shell interactions) have $\nabla^2\rho_{bcp} > 0$ and low ρ_{bcp}. Intermediate bonds are associated with $\nabla^2\rho_{bcp} > 0$ and low to medium ρ_{bcp}, i.e., values between shared and closed-shell interactions. On the other hand, Cremer and Kraka (41, 42) have shown that for covalent and intermediate bonds the energy density H_{bcp} has negative values. Another parameter used to describe a bond is the ellipticity (ε) that demonstrates whether the electronic charge is preferentially accumulated in a given direction between two bonded atoms. Sigma bonds have $\varepsilon = 0$, while double or π bonds, in general, have $\varepsilon > 0$.

COMPUTATIONAL DETAILS

All calculations and geometry optimizations were performed by using the Gaussian-94 program (43) at a DFT (density functional theory) level using Becke's three-parameter hybrid functional (44) and Lee, Yang, and Parr's correlation functional (45) (B3LYP). The basis sets and the relativistic compact effective potentials, which include $(n-1)s^2$, $(n-1)p^6$, $(n-1)d^x$, and $(n)s^y$ electrons from Stevens *et al.* (46), were used for Fe, Co, Ni, Cu, and Zn atoms. The all-electron 6–311G(d, p) for N and O and 6–31G(d, p) for Al, Si, and H basis sets, provided by the Gaussian-94 package, were employed. The electronic charge distribution of the catalyst models was analyzed using the natural bond orbital (NBO) partition scheme (47, 48) and the topological properties of the electronic density of the bonds (EXTREME program) (49). In all calculations the symmetry of the models used was C2, and the total charge of the *M*-T3 complex was set according to the lowest formal oxidation state of the metallic ion. For all complexes the spin state was given by the number of unpaired electrons on the metallic center.

For the free NO_2 molecule, the calculated N–O bond length and O–N–O angle are 1.19 Å and 134.2°, respectively, in good agreement with the experimental values of 1.19 Å and 133.9° (50). For the free NO_2^- molecule, the calculated values of the N–O bond length and O–N–O angle (1.27 Å, 116.0°) are similar to the experimental values of 1.25 Å and 117.5° (51).

RESULTS AND DISCUSSION

Table 1 shows the geometrical properties as well as the calculated binding energy for NO_2 adsorption on the Cu-T3 model. Figure 2 displays the optimal structure of the NO_2Cu-T3 complex obtained by an optimization procedure. In this optimal structure the NO_2 molecule is parallel to the O–Al–O atoms of the T3 site model. In general, the results are in good agreement with those previously published (14). The data in Table 1 show that the interaction of the NO_2 molecule with the Cu atom produces an enlargement of the N–O distance (N–O_3), from 1.19 to 1.26 Å and a reduction of the natural angle (O_3–N–O_3), from

TABLE 1

Bond Distances and Angles of the Cu–T3 and NO_2Cu–T3 Structures and Free NO_2 and NO_2^- Molecules[a]

	Cu-O (Å)	Angle O–Cu–O	N-O_3 (Å)	Angle O_3–N–O_3	O_3-Cu (Å)	ΔE^b (kcal/mol)
Cu-T3	2.00	83.2				
	1.99[c]					
NO_2Cu-T3	1.94	80.6	1.26	110.9	2.02	43.3
	1.94[c]		1.26[c]	110.5[c]	2.01[c]	42.7[c]
Free NO_2			1.19	134.2		
Free NO_2^-			1.27	116.0		

[a] T3 = $H_3SiOAl(OH)_2OSiH_3$.
[b] Calculated binding energy.
[c] Reference 11.

134.2 to 110.9°, of the free NO_2 molecule. The geometrical properties of adsorbed NO_2 are similar to those of the free ion NO_2^-, which is an indication of a charge transfer from the metal to the NO_2. Table 2 shows that the Cu atom attached to the zeolite model (Cu-T3) has a net charge (Q_{Cu}) of $+0.88e$ with an electronic population that corresponds to a d^{10} closed-shell structure. After the interaction with the NO_2 molecule, in the final complex (NO_2Cu-T3), the Cu atom presented a d^9 configuration with a net charge of $+1.33e$, while the NO_2 was negatively charged ($Q_{NO_2} = -0.60e$). These results are in agreement with the mechanism proposed by Sauer and co-workers (14) which explains the bond formation between the Cu^+ and the NO_2 molecule. Since there is a charge transfer from the Cu-T3 complex to the NO_2 molecule, the calculations were repeated with the addition of diffuse functions to the basis set. The results show that there are no important changes either in the geometry or in the calculated binding energies when using diffuse functions. For example, the O_3–N–O_3 angle changes from 110.9 to 110.7°; and the O–*M*–O angle changes from 80.6 to 80.7°. The calculated binding energy decreases from 43.3 to 41.0 kcal/mol. Therefore diffuse functions were not included in the calculations.

According to Sauer (14) an electronic promotion from the $3d^{10}$ configuration to the $3d^94s^1$ configuration is necessary to produce a bond between the Cu^+ and the NO_2 molecule. In the excited state, d^9s^1, the Cu atom has two unpaired electrons and interacts with the unpaired electron of the NO_2 molecule forming the bond. The bond between the NO_2 molecule and the metal is produced using the 4s electron of the metal atom; the second unpaired electron of the metal remains in the d orbital. In our particular case it is localized in the 3dyz orbital, as shown in Table 2. The electronic charge transfer from the Cu ion to the NO_2 molecule increases the positive charge on this atom and therefore increases the electrostatic interactions of the metal with the negatively charged zeolite, reducing the Cu–O distance and stabilizing the ion. The stabilization is due, in part, to the fact that the 3d–4s promotions reduce the Pauli repulsion between Cu and O atoms and the electron–electron repulsion between the 3d electrons (14, 36). Besides these effects, the zeolite helps to reduce the energy gap between d^9s^1 and d^{10} states, which facilitates the NO_2 adsorption. As a matter of fact, the calculations show that for a single Cu^+ ion the d^9s^1 state is 55.9 kcal/mol higher in energy than the d^{10} state, but when Cu^+ is attached to the zeolite framework this difference is only 39.5 kcal/mol.

TABLE 2

Electronic and Topological Properties of the Electronic Density[a] of the Cu-T3 and NO_2Cu–T3 Structures and the NO_2 and NO_2^- Molecules

	Q_{NO_2}	Q_{Cu}	4sp	3dxy	3dxz	3dyz	3dx^2-y^2	3dz^2
Cu-T3	—	+0.88	0.18	2.00	2.00	1.98	1.97	1.99
NO_2Cu-T3	−0.60	+1.33	0.41	2.00	1.99	1.31	1.98	1.98

	Bond	ρ_{bcp}	H_{bcp}	$\nabla^2\rho_{bcp}$	ε
Cu-T3	Cu–O	0.078	−0.016	0.386	0.016
	Cu–O	0.086	−0.018	0.431	0.027
NO_2Cu-T3	Cu–O_3	0.075	−0.016	0.327	0.102
	N–O_3	0.458	−0.571	−1.012	0.084
NO_2^-	N–O_3	0.451	−0.545	−0.922	0.073
NO_2	N–O_3	0.525	−0.733	−1.220	0.053

[a] ρ_{crit} is the electronic density at the bcp; H_{crit} is the energy density at the bcp; $\nabla^2\rho_{crit}$ is the Laplacian of $\rho(r)$ at the bcp.

The topological properties of the molecular electronic density ρ at the bcp show that the interaction between Cu and oxygen atoms can be classified as closed-shell or intermediate interactions. The molecular electronic density at the bcp (ρ_{bcp}) is low, the Lapacian ($\nabla^2\rho_{bcp}$) is positive, and the energy density H_{bcp} has a negative value. Previously published results (52–55) show that in general, the metal–oxygen interaction is characterized by positive values of $\nabla^2\rho_{bcp}$. The ellipticity values (ε) suggest a degree of π character for the metal–O bond (52, 55).

In the case of the NO_2 and NO_2^- free molecules, the topological properties show that the N–O bond (N–O_3) is a classical covalent bond (shared interaction). The positive values of ε can be rationalized considering that the HOMO orbital of these molecules has a strong contribution to the p_z atomic orbital of the N and O atoms, and therefore some π character is present in the N–O bond. Due to the increase of the N–O bond length (N–O_3) in the final complex with the Cu atom (NO_2Cu-T3), the electronic density as well as the degree of local charge concentration, measured by the $\nabla^2\rho_{bcp}$ values, are lower in the complex than in the NO_2 free molecule. The topological properties of the N–O_3 bond are similar to those in the NO_2Cu-T3 complex and NO_2^- molecule, which demonstrates that the adsorbed NO_2 molecule is topologically equivalent to the NO_2^- free molecule.

The bonding mechanism, previously discussed for the interaction of NO_2 with the Cu–T3 complex, is not general, and it is expected that different mechanisms operate with other transition metals. To investigate the general mechanism of the interaction of the NO_2 molecule with metallic ions, other metals such as Zn, Ni, Co, and Fe were studied. The adsorption modes of the NO_2 molecule, where the two O atoms interact directly with the metallic center, were found to be more stable than the modes where the N atom interacts with the metal. Figures 2 and 3 display the general structures obtained for the parallel (NO_2M-T3$\parallel$) and perpendicular (NO_2M-T3$\perp$) adsorption modes of the NO_2 on *M*-T3 systems (*M* = Zn, Cu, Ni, Co, and Fe). As shown in Table 3, the calculated binding energies for the Zn-T3 system are higher than those corresponding to the Cu-T3 system. In contrast to the Cu-T3 system, in the Zn-T3 system the perpendicular adsorption mode is slightly more favored than the parallel mode. Table 4 shows that before NO_2 adsorption, the Zn atom has an electronic distribution

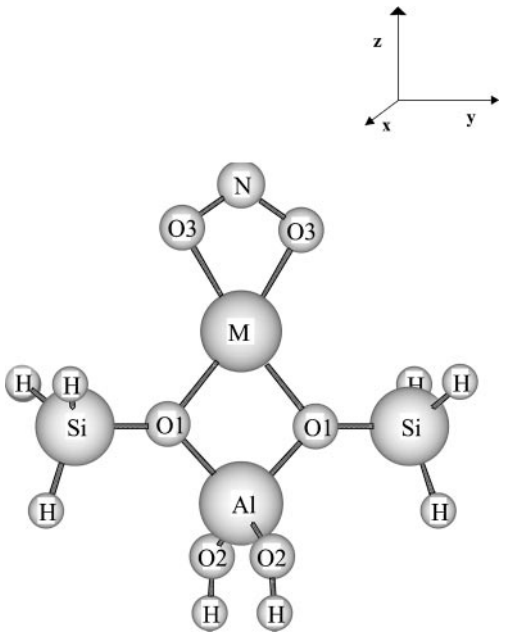

FIG. 2. Schematic representation of the NO_2M–T3 structure (M = Zn, Cu, Ni, Co, Fe). NO_2 is located in the plane of the Al and the O1 atoms.

TABLE 3
Bond Distances and Angles of M-T3, NO_2M-T3⊥ and NO_2 M-T3∥ Structures[a]

M-T3 NO_2M-T3	M–O (Å)	Angle O–M–O	N–O_3 (Å)	Angle O_3–N–O_3	O_3–M (Å)	ΔE^b (kcal/mol)
Zn-T3	2.04	78.1	—	—	—	—
NO_2Zn-T3⊥	1.97	80.9	1.26	113.0	2.09	64.7
NO_2Zn-T3∥	1.98	80.0	1.25	113.0	2.12	61.6
Cu–T3[c]	2.00	83.2	—	—	—	—
NO_2Cu-T3∥	1.94	80.6	1.26	110.9	2.02	43.2
NO_2Cu-T3⊥	2.00	79.5	1.26	109.9	2.00	27.9
Ni-T3	1.96	83.9	—	—	—	—
NO_2Ni-T3∥	1.96	79.3	1.26	111.6	2.07	52.0
NO_2Ni-T3⊥	1.96	79.1	1.27	111.3	2.05	50.7
Co-T3	1.86	87.1	—	—	—	—
NO_2Co-T3∥	1.81	83.0	1.28	108.1	1.92	20.0
NO_2Co-T3⊥	2.04	77.3	1.27	111.0	2.04	13.6
Fe-T3	1.90	85.3	—	—	—	—
NO_2Fe-T3∥	1.88	84.8	1.27	109.9	2.07	33.8
NO_2Fe-T3⊥	1.87	86.0	1.28	106.9	1.93	12.2

[a] T3 = $[H_3SiOAl(OH)_2OSiH_3]$; M = Zn, Cu, Ni, Co, and Fe.
[b] Calculated binding energy.
[c] Included to facilitate the discussion.

that corresponds to a $4s^13d^{10}$ configuration ($4s^{1.14}3d^{10.0}$). After the adsorption in the NO_2Zn-T3 complexes, the Zn^+ ion shares the 4s electron with the NO_2 molecule and adopts a $4s^{0.5}3d^{9.98}$ configuration. These results indicate that the interaction takes place mainly through the 4s electron of the Zn^+ ion. Therefore, the perpendicular and parallel adsorption modes have similar total energies (see Table 3); consequently, the NO_2 molecule can rotate freely around an imaginary axis that connects the Al, Zn, and N atoms. As a matter of fact, the rotational energy barrier between two NO_2Zn-T3⊥ structures is small, 3.1 kcal/mol, and the maximum corresponds to the NO_2Zn-T3∥ structure (see Fig. 4).

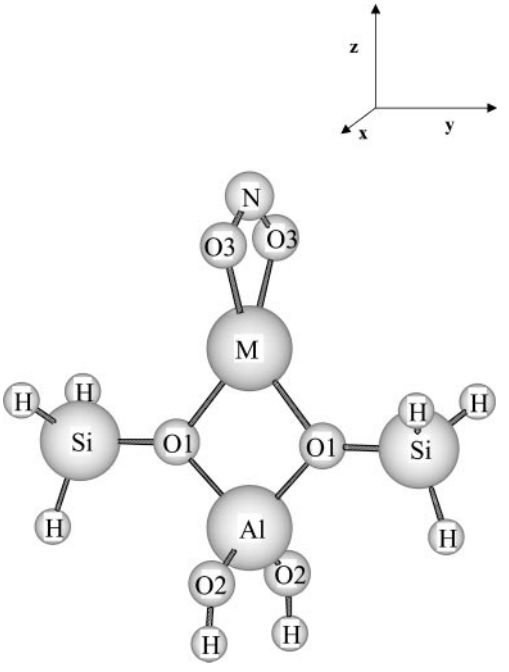

FIG. 3. Schematic representation of the NO_2M-T3⊥ structure (M = Zn, Cu, Ni, Co, Fe). NO_2 is located in the perpendicular plane to the Al and O1 atoms.

TABLE 4
NBO Electronic Population of the M-T3 and NO_2 M-T3 Complexes[a]

M-T3 NO_2M-T3	Q_{NO_2}	Q_M	4sp	3dxy	3dxz	3dyz	3dx^2-y^2	3dz^2
Zn-T3	—	+0.86	1.14	2.00	2.00	2.00	2.00	2.00
NO_2Zn-T3⊥	−0.67	+1.50	0.50	2.00	2.00	1.99	2.00	1.99
NO_2Zn-T3∥	−0.66	+1.49	0.51	2.00	2.00	2.00	1.99	1.99
Cu-T3	—	+0.88	0.18	2.00	2.00	1.98	1.97	1.99
NO_2Cu-T3∥	−0.60	+1.33	0.41	2.00	1.99	1.31	1.98	1.98
NO_2Cu-T3⊥	−0.55	+1.34	0.40	2.00	1.30	1.98	2.00	1.98
Ni-T3	—	+0.80	0.29	2.00	1.99	1.06	1.89	1.97
NO_2Ni-T3∥	−0.65	+1.36	0.42	2.00	1.05	1.21	1.98	1.98
NO_2Ni-T3⊥	−0.64	+1.35	0.38	2.00	1.16	1.13	2.00	1.98
Co-T3	—	+1.48	0.24	1.09	1.07	1.15	1.98	1.99
NO_2Co-T3∥	−0.38	+1.51	0.37	1.17	1.14	0.86	1.98	1.97
NO_2Co-T3⊥	−0.60	+1.39	0.42	1.03	1.13	1.07	1.99	1.97
Fe-T3	—	+1.57	0.21	1.06	1.07	1.10	1.46	1.53
NO_2Fe-T3∥	−0.55	+1.84	0.33	1.23	1.15	1.27	1.06	1.08
NO_2Fe-T3⊥	−0.30	+1.58	0.36	1.10	0.91	1.17	1.38	1.50

[a] M = Zn, Cu, Ni, Co, Fe.

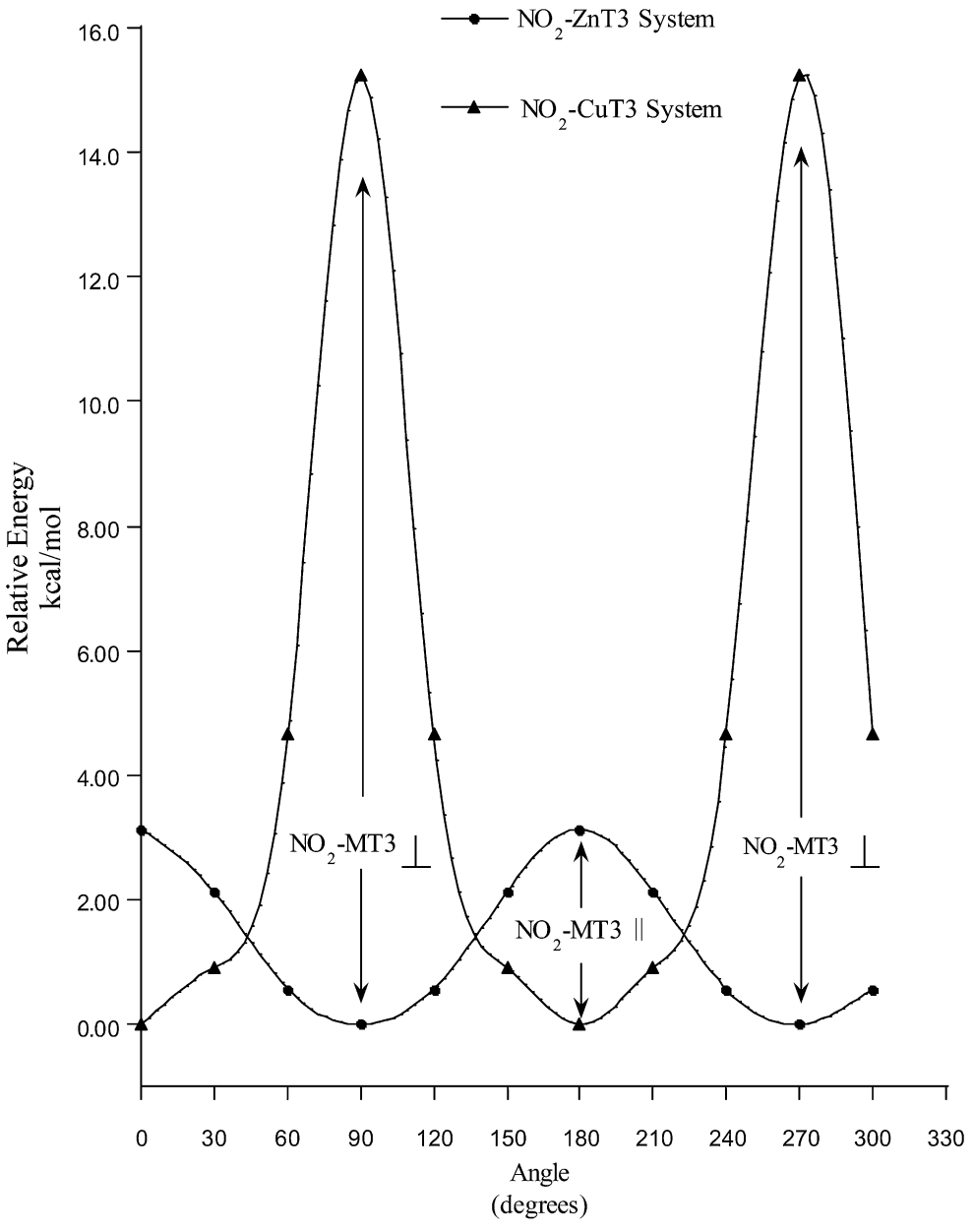

FIG. 4. Rotational energy curves for the NO_2Zn-T3 and NO_2Cu-T3 systems.

Since the 4s electron is available in the Zn-T3 for bonding, the mechanism of the electronic promotion is not necessary.

According to our results, when the NO_2 molecule approaches the Cu–T3 system, there is an excitation of one d electron to the 4s orbital. This promotion occurs in the d orbital that diminishes the electron–electron repulsion between the electrons of the oxygen atoms that belong to the NO_2 molecule and the d electrons of the metallic ion. Therefore for the parallel adsorption mode (NO_2Cu-T3$\|$), where the NO_2 molecule is in the *yz* plane (see Fig. 2), the promoted electron belongs to the 3d*yz* orbital (see Table 4) reducing the electron–electron repulsion between the oxygen electrons and the d electrons of the metal, as shown schematically in Fig. 5. For the perpendicular adsorption mode (NO_2Cu-T3$\perp$), the NO_2 molecule is in the *xz* plane (see Fig. 3). Consequently, in the final structure, the unpaired electron is located in the 3d*xz* orbital. The NO_2Cu-T3$\perp$ has a higher energy than the NO_2Cu-T3$\|$ complex, because in the former the electron–electron repulsions between the electrons of the double-occupied 3d*yz* orbital and the electrons of the oxygen atoms of the T3 structure are higher than those in the NO_2Cu-T3$\|$ complex, which has a single-occupied 3d*yz* orbital. Consequenly, the rotational potential energy has a maximum at 90 and 270°, which corresponds to the NO_2Cu-T3$\perp$ structures, as shown in Fig. 4.

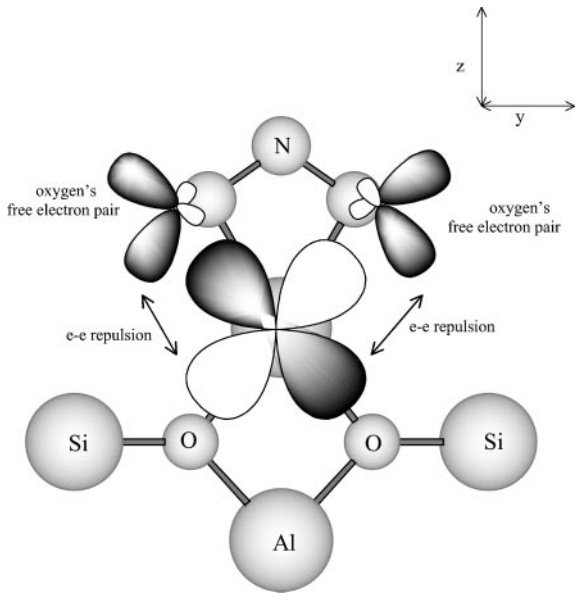

FIG. 5. Schematic representation of the electronic repulsion between the 3dyz electrons of the metal and the electrons of the oxygen of the NO_2 molecule.

Table 5 shows that the topological properties of the zinc–oxygen (Zn–O and Zn–O_2) and copper–oxygen (Cu–O and Cu–O_2) bonds are similar, i.e., low ρ_{bcp}, positive $\nabla^2 \rho_{bcp}$ negative H_{bcp}, and $\varepsilon > 0$. Therefore, the topological analysis of the electron density gives qualitatively the same picture for the NO_2Cu-T3 and NO_2Zn-T3 complexes. This fact and the results of the NBO analysis indicate that the bond between the NO_2 molecule and the metallic ion can be explained in terms of the interaction of the metal 4s electron and the electron of the NO_2 HOMO orbital, which produces a two-electron two-bond complex.

TABLE 5

Topological Properties of the Electronic Density[a] of the *M*-T3 and NO_2*M*-T3 Complexes[b]

	Bond	ρ_{bcp}	H_{bcp}	$\nabla^2\rho_{bcp}$	ε
Zn-T3	Zn–O	0.069	−0.012	0.325	0.034
	Zn–O	0.080	−0.017	0.400	0.030
NO_2Zn-T3⊥	Zn–O_3	0.066	−0.012	0.272	0.077
	N–O_3	0.464	−0.587	−1.041	0.077
Cu-T3	Cu–O	0.078	−0.016	0.386	0.016
	Cu–O	0.086	−0.018	0.431	0.027
NO_2Cu-T3‖	Cu–O_3	0.075	−0.016	0.327	0.102
	N–O_3	0.458	−0.571	−1.012	0.084
Ni-T3	Ni–O	0.078	−0.010	0.470	0.126
	Ni–O	0.084	−0.013	0.439	0.235
NO_2Ni-T3‖	Ni–O_3	0.069	−0.012	0.287	0.122
	N–O_3	0.458	−0.569	−1.003	0.077
Co-T3	Co–O	0.109	−0.010	0.667	0.332
	Co–O	0.126	−0.018	0.696	0.256
NO_2Co-T3‖	Co–O_3	0.100	−0.008	0.491	0.120
	N–O_3	0.446	−0.542	−0.961	0.081
Fe-T3	Fe–O	0.102	−0.011	0.624	0.291
	Fe–O	0.112	−0.016	0.639	0.155
NO_2Fe-T3‖	Fe–O_3	0.076	−0.008	0.311	0.080
	N–O_3	0.454	−0.564	−1.002	0.071

[a] ρ_{crit}, electronic density at the bcp; H_{crit}, energy density at the bcp; $\nabla^2\rho_{crit}$, Laplacian of $\rho(r)$ at the bcp. ε, ellipticity values of the bond.
[b] M = Zn, Cu, Ni, Co, Fe.

As shown in Table 3, after the adsorption of NO_2, the N–O_3 distance increases and the natural angle O_3–N–O_3 decreases, and there is a charge transfer from the metal to the NO_2 molecule (see Table 4) which favors the electrostatic interaction between the NO_2 molecule and the metallic center. According to the NBO analysis of the Ni complexes, the promotion mechanism 3d → 4s seems to be necessary to explain the bonding mechanism. In fact, in the Ni-T3 complex, the Ni atom has a $3d^9$ configuration ($4s^{0.3}3d^{8.9}$) with the unpaired electron located in the 3dyz orbital. After the interaction with NO_2, in NO_2Ni-T3‖ as well as in NO_2Ni-T3⊥, the Ni ion has a $3d^8$ configuration ($4s^{0.4}3d^{8.2}$) with the unpaired electrons in the 3dyz and 3dxz orbitals. The promotion 3d → 4s helps to reduce not only the electron–electron repulsion between the d electrons of the Ni ion and the electron pairs of the oxygen atoms but also the repulsion between the 3d electrons.

Calculations for the naked Ni^+ ion show that the $4s^13d^8$ state is 57.2 kcal/mol higher in energy than the $3d^9$ state. In the Ni-T3 complex, there is only a 26.8 kcal/mol energy difference. Therefore, the support reduces the energy difference between the $3d^9$ and the $4s^13d^8$ configuration facilitating NO_2 adsorption. In system where the Ni atom has two unpaired electrons, and one of them is in the plane where the NO_2 molecule is localized, other electronic distributions are possible, for example, those where the extra electron is localized in the 3dxy orbital. The other electronic distributions are higher in energy than the 3dxy^2, 3dxz^1, and 3dyz^1 orbitals, due to the electronic repulsion between double-occupied 3dxz or 3dyz orbitals and the electrons of the oxygen atoms.

A different bonding pattern arises from the analysis of the Co and Fe complexes. The calculated binding energies for both complexes are lower than those corresponding to the Zn, Cu, or Ni complex (see Table 3), and for both metals the net charge is close to the formal charge of +2. Moreover, the charge transfer from the metal (M = Co, Fe) to the NO_2 molecule in the NO_2M-T3 complexes is small in comparison to the other complexes (M = Zn, Cu, Ni). There is a strong rearrangement of the electronic population of the d orbitals; however, the total electronic configuration of the metallic ion does not change. For example, the Co ion has a $3d^7$ configuration in the Co-T3, NO_2Co-T3‖, and NO_2Co-T3⊥ complexes ($4s^{0.2}3d^{7.3}$, $4s^{0.4}3d^{7.1}$, and $4s^{0.4}3d^{7.2}$, respectively), and the Fe ion has a $3d^6$ configuration ($4s^{0.2}3d^{6.2}$ for Fe-T3, $4s^{0.3}3d^{5.8}$ for NO_2Fe-T3‖ and $4s^{0.4}3d^{6.1}$ for NO_2Fe-T3⊥). On the other hand, the charge transfer from Co-T3 or Fe-T3 to the NO_2 molecule, −0.38e and −0.55e, respectively, is greater than the change in the net charge of the ions (0.03e and 0.27e for Co and Fe, respectively). For

Co-T3 and Fe-T3 systems, the adsorption in the parallel plane is favored over that in the perpendicular plane. The analyses of these results indicate that first, a charge transfer from the zeolite framework to the metallic ion must occur to compensate for the charge transfer from the metallic ion to the NO_2 molecule. Second, the electrostatic interactions have an important participation in the formation of the bond between either Fe^{2+} or Co^{2+} and NO_2^-.

It is well known from experimental results (23) that the Co ions, in Co-ZSM-5, have an oxidation state of +2 and are not easily reducible to Co^+ or oxidable to Co^{3+}. Our results are in agreement with these experimental facts. According to Table 4 there is no change in the net charge of the Co ion after NO_2 adsorption; therefore Co^{2+} is not reduced or oxidized by the adsorption. Armor and co-workers (23) in an experimental work on Co-ferrierite and Co-zeolite catalysts suggested that in the mechanism of the SCR of NO_x, the formation of an adsorbed NO_2 on Co^{2+} is a necessary step. After adsorption, the CH_4 molecule interacts with the NO_2(ad) molecule forming a $CH_3\cdot$ free radical which interacts with another NO_2(ad) molecule, and the reaction proceeds followed by subsequent transformations (19, 20, 23). The electronic distribution of Co in the NO_2Co-T3‖ complex (see Table 4) suggests that it is possible to bond other molecules to Co^{2+} in the perpendicular plane to the NO_2 molecule, because the free unpaired electron is located in the 3dxz orbital. Therefore the $CH_3\cdot$ radical, or other molecules such as NO, can react with this electron, and structures where CH_3 and NO_2 are simultaneously bonded to the Co atom are possible, as shown in Fig. 6. These types of structures, regarding the interaction of NO with NO_2Cu-T3‖, have been proposed in the literature (37) .

Joyner and Stockenhuber (56), in an experimental study using X-ray adsorption spectroscopy and EXAFS, proposed that the structure of the iron in the Fe-ZSM-5 catalysts is an iron–oxygen cluster analogous to ferredoxin. Calculations made on this type of cluster (see Fig. 7) show the same trend found for NO_2Fe-T3 complexes; i.e., there is a charge transfer from the cluster to the NO_2 molecule ($Q_{NO_2} = -0.52$ in NO_2–Fe_3O_4). The Fe 4sp orbitals participate in the NO_2–Fe bond, and the Fe–O_3 distance (1.90 Å) is similar to the Fe–O_3 distance found in the NO_2Fe-T3 complex.

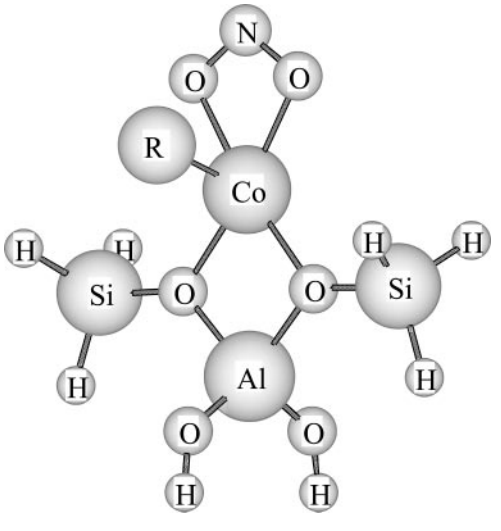

FIG. 6. Schematic representation of a possible structure where NO_2 and the R fragment (R=CH_3, NO, etc.) are simultaneously bonded to the Co atom.

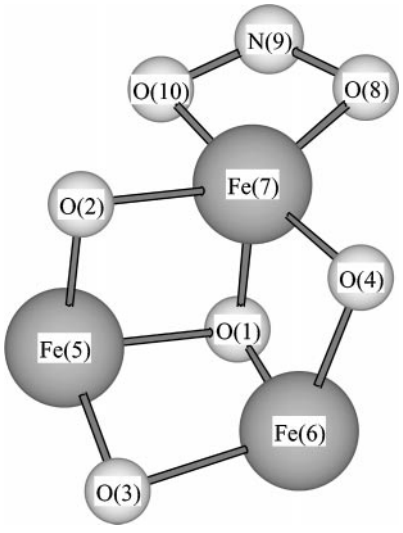

FIG. 7. Schematic representation of the NO_2–Fe_3O_4 cluster.

CONCLUSIONS

The structures, binding energies, and topological properties of the bonds have been determined for M-T3 and NO_2M-T3 systems (M = Fe, Co, Ni, Cu, and Zn). The coordination mode of NO_2 through the two oxygen atoms to the metallic center is the most stable, while other coordination modes are less stable. This agrees with previously published results (14, 29, 33–35) which show that, in general, the η^2-O,O structure is optimal when NO_2 binds to a metallic ion attached to a zeolite framework. In general, a charge transfer from the metal to the NO_2 molecule and a weakening of the N–O bond occur. The charge transfer increases the electrostatic interactions of the metal with the negatively charged zeolite, reducing the metal–O (ZSM-5) distance. The bonding in NO_2M-T3 can be described in terms of the metal 4s orbital and the NO_2 HOMO orbital. Therefore an unpaired electron in the 4s orbital of the metal is necessary to produce the bond. The bonding mechanism of Sauer and co-workers (14) explains the interaction of NO_2 with Cu^+ and Ni^+, but not with Zn^+, Co^{2+}, or Fe^{2+}.

The topological properties of the N–O_3 bond are similar in all the NO_2M-T3 complexes studied here and closer to the properties of the NO_2^- ion. Therefore, the weakening

of the N–O bond in the NO_2 molecule (N–O_3) could be explained in terms of a charge transfer from the complex *M*-T3 to the HOMO orbital of NO_2.

ACKNOWLEDGMENTS

The authors gratefully acknowledge CONIPET (Grant 97003734) and CONICIT (Grant S1-96001399) for financial support.

REFERENCES

1. Bell, A. T., *Catal Today* **38**, 151 (1997).
2. Zhu, Z., Liu, Z., Niu, H., Liu, S., Hu, T., Liu, T., and Xie, Y., *J. Catal.* **197**, 6 (2001).
3. Maunula, T., Ahola, J., and Hamada, H., *Appl. Catal. B Environ.* **26**, 173 (2000).
4. Iwamoto, M., *Stud. Surf Sci. Catal.* **54**, 121 (1990).
5. Sato, S., Yu, Y., Yahiro, H., Mizuno, N., and Iwamoto, M., *Appl. Catal.* **70**, L1 (1991).
6. Iwamoto, M., and Yahiro, H., *Catal. Today* **22**, 5 (1994).
7. Iwamoto, M., Yahiro, H., and Mine, Y., *Chem. Lett.* **2**, 213 (1989).
8. Held, W., Koenig, A., Richter, T., and Puppe, L., SAE Tech. Paper Ser. 900, 496 (1990).
9. Shelef, M., *Chem. Rev.* **95**, 209 (1995).
10. Iwamoto, M., Yahiro, H., Tanda, K., Mizuno, N., Mine, Y., and Kagawa, S. J., *Phys. Chem.* **95**, 3727 (1991).
11. Li, Y., and Hall, W. K., *J. Catal.* **129**, 202 (1991).
12. Spoto, G., Zecchina, A., Bordiga, S., Ricchiardi, G., Martra, G., Leofanti, G., and Petrini, G., *Appl. Catal. B* **3**, 151 (1994).
13. Wichterlová, B., Dedecek, J., Sobalík, J., Vondrová, Z., and Klier, K., *J. Catal.* **169**, 194 (1997).
14. Rodriguez-Santiago, L., Sierka, M., Branchadell, V., Sodupe, M., and Sauer, J., *J. Am. Chem. Soc.* **120**, 1545 (1998).
15. Misono, M., and Kondo, K., *Chem Lett.* 1001 (1991).
16. Yokoyama, C., and Misono, M., *Chem Lett.* 1669 (1992).
17. Yokoyama, C., and Misono, M., *Bull. Chem. Soc. Jpn.* **67**, 557 (1994).
18. Yokoyama, C., and Misono, M., *J. Catal.* **150**, 9 (1994).
19. Lukyanov, D., Lombardo, E., Sill, G., D'Itri, J., and Hall, W. K., *J. Catal.* **163**, 447 (1996).
20. Lombardo, E., Sill, G., D'Itri, J., and Hall, W. K., *J. Catal.* **173**, 440 (1998).
21. Li, Y., and Armor, J. N., *Appl. Catal. B* **2**, 239 (1993).
22. Li, Y., and Armor, J. N., *Appl. Catal. B* **1**, L31 (1992).
23. Li, Y., Salger, T. L., and Armor, J. N., *J. Catal.* **150**, 388 (1994).
24. Feng, X., and Hall, W. K., *J. Catal.* **166**, 368 (1997).
25. Joyner, R. W., and Stockernhuber, M., *Catal. Lett.* **45**, 15 (1997).
26. Hall, W. K., Feng, X., Dumesic, J., and Watwe, R., *Catal. Lett.* **52**, 13 (1998).
27. Volodin, A. M., Sobolev, V. I., and Zhidomirov, G. M., *Kinet. Catal.* **39**, 775 (1998).
28. Himey, H., Yamada, M., Kubo, M., Vetrtivel, R., Broclwik, E., and Miyamoto, A., *J. Phys. Chem.* **99**, 12,461 (1995).
29. Rodríguez-Santiago, L., Branchadell, V., and Sodupe, M., *J. Chem. Phys.* **103**, 9738 (1995).
30. Yokomichi, Y., Yamabe, T., Ohtsuka, H., and Kakumota, T., *J. Phys. Chem.* **100**, 14, 424 (1996).
31. Kanougi, T., Furukawa, K., Yamadaya, M., Oumi, Y., Kubo, M., Stirling, A., Fahmi, A., and Miyamoto, A., *App. Surf. Sci.* **119**, 103 (1997).
32. Stirling, A., *Chem. Phys. Lett.* **298**, 101 (1998).
33. Rodríguez-Santiago, L., Solans-Monfort, X., Sodupe, M., and Branchadell, V., *Inorg. Chem.* **37**, 4512 (1998).
34. Rodríguez-Santiago, L., Sodupe, M., and Branchadell, V., *J. Phys. Chem. A* **102**, 630 (1998).
35. Lu, X., Xu, X., Wang, N., and Zhang, Q., *J. Phys. Chem. A* **103**, 10,969 (1999).
36. Nachtigall, P., Nachtigallova, D., and Sauer, J., *J. Phys. Chem. B* **104**, 1738 (2000).
37. Solans-Monfort, X., Branchadell, V., and Sodupe, M., *J. Phys. Chem. A* **104**, 3225 (2000).
38. Bader, R. W. F., *Chem. Rev.* **91**, 893 (1991).
39. Bader, R. W. F., *in* "Atoms in Molecules: A Quantum Theory" (J. Halpern and M. L. H. Green, Eds.), Chap. 1, p. 248. Clarendon Press, Oxford, 1990.
40. Bader, R. W. F., Essen, H., *J. Chem. Phys.* **80**, 1943 (1984).
41. Cremer, D., and Kraka, E., *Angew. Chem. Int. Ed. Engl.* **109**, 5917 (1984).
42. Cremer, D., and Kraka, E., *Angew. Chem. Int. Ed. Engl.* **23**, 627 (1984).
43. Frish, M. J., Trucks, G. W., Schlegel, H. B., Gill, P. M. W., Johnson, B. G., Robb, M. A., Cheeseman, J. R., Keith, T., Petersson, G. A., Montgomery, J. A., Raghavachari, K., Al-Laham, M. A., Zakrzewski, V. G., Ortiz, J. V., Foresman, J. B., Cioslowski, J., Stefanov, B. B., Nanayakkara, A., Challacombe, M., Peny, C. Y., Ayala, P. Y., Chen, W., Wong, M. W., Andres, J. L., Replogle, E. S., Gomperts, R., Martin, R. L., Fox, D. J., Binkey, J. S., Defrees, D. J., Baker, J., Stewart, P. J., Head-Gordon, M., Gonzales, C., and Pople, J. A., Gaussian 94, Revision D. 4. Gaussian, Inc., Pittsburgh, PA, 1995.
44. Becke, A. D., *J. Chem. Phys.* **98**, 5648 (1993).
45. Lee, C., Yang, W., and Parr, R. G., *Phys. Rev. B* **37**, 785 (1988).
46. Stevens, W., Basch, H., and Krauss, M. J., *Chem. Phys.* **81**, 6026 (1984).
47. Glendening, E. D., Reed, A. E., Carpenter, J. E., and Weinhold, F., NBO Version 3.1. Gaussian-94 Programs Package. Gaussian, Inc., Pittsburgh, PA, 1995.
48. Reed, A. E., Curtiss, L. A., and Weinhold, F., *Chem. Rev.* **88**, 899 (1988).
49. Biegler-Koning, F. W., Bader R. F. W., and Tang, T. H., *J. Comp. Chem.* **3**, 317 (1982).
50. Morino, Y., Tawimoto, M., Saito, S., Hirota, E., Awata, R., and Tanaka, T., *J. Mol. Spectrosc.* **98**, 331 (1983).
51. Ervin, K. M., Ho, J., and Lineberger, W. C., *J. Chem. Phys.* **92**, 5404 (1988).
52. Kempf, J., Rohmer, M., Poblet, J., Bo, C., and Bénerd, M., *J. Am. Chem. Soc.* **114**, 1136 (1992).
53. Gillespie, R., Bytheway, I., Tang, T., and Bader, R. F. W., *Inorg. Chem.* **35**, 3954 (1996).
54. Sierraalta, A., and Ruette, F., *J. Comp. Chem.* **15**, 313 (1994).
55. Sierraalta, A., *Chem. Phys. Lett.* **227**, 557 (1994).
56. Joyner, R. W., and Stockenhuber, M., *Catal. Lett.* **45**, 15 (1997).